# Novel Subarray Partition Algorithm for Solving the Problem of Too Low Beam Collection Efficiency Caused by Dividing a Few Subarrays

**Jianxiong Li[1, 2], Ziyu Han[1, 2], and Cuijuan Guo[1, 2, *]**

**Abstract**—Beam Collection Efficiency ($BCE$), sidelobe level outside the receiving area ($CSL$), and cost are need to be considered in optimizing the transmitting array of a Microwave Wireless Power Transmission (MWPT) system. To solve the problem of too low $BCE$ caused by dividing a small number of subarrays, this paper proposes a novel one-step subarray partition algorithm named Multi-Particle Multi-Parameter Dynamic Weight Particle Swarm Optimization Subarray Partition (MPMP-DWPSO-SP). The algorithm optimizes the position and structure of each element at the same time, and the number of the subarrays is no more than 4. It is verified by simulation that the $BCE$ obtained by using this algorithm to optimize the Sparse Quadrant Symmetrical Rectangular Array (SQSRA) with an aperture of $4.5\lambda \times 4.5\lambda$ and the array element number of $8 \times 8$ can reach more than 90%. In addition, a new intelligent optimization model is designed for dividing the $8 \times 8$ array into 2 subarrays, and $BCE$ and $CSL$ can reach 91.69% and $-17.61$ dB.

## 1. INTRODUCTION

Microwave Wireless Power Transmission (MWPT) is a technology using microwaves to achieve long-distance energy transmission [1]. It is widely used to power distributed electronic devices [2], power sensors and actuators [3], space solar satellites [4], and other fields. The goal of improving power transmission efficiency has been widely researched in recent years. Among them, Beam Collection Efficiency ($BCE$) is one of the most essential parameters of the MWPT system. It is defined as the ratio of the energy captured by the receiving antenna to the energy radiated by the transmitting antenna [5]. Additionally, sidelobe level outside the receiving area ($CSL$) is another key index, which is defined as the highest side-lobe level outside the receiving area. Studies have shown that the Gaussian distribution of continuous aperture antenna is close to the optimal distribution and the maximum $BCE$ can be obtained [3]. However in practice, the Gaussian distributed array needs to be equipped with amplifiers and phase shifters for each element separately, which leads to high cost. It will also make the array structure and feeding network extremely complicated, so it is very necessary to design an effective array optimization algorithm to optimize the feeding network and improve $BCE$ simultaneously.

Subarray partition technology is an array design technology that lowers the hardware cost and algorithm complexity by reducing the dimensionality of the signal processing algorithm at the elementary level to the subarray level [6]. The nonuniform non-overlapping partition method is more effective in improving $BCE$ and reducing cost. For the transmitting array, designing a reasonable subarray structure is of great research value. The difference in the subarray structure will directly affect the performance of the subarray-level signal processing [7]. Previous studies have divided subarrays by using excitation [8]. The optimization of the subarray partition is divided into two steps: the first step is optimizing the position of the element and the second step is dividing subarrays [9], or the first step is optimizing the

structure of the subarray, and the second step is optimizing the element position [10–11]. The obtained *BCE* by using this method can achieve satisfactory results when it is divided into multiple subarrays (more than 8), but when the number of subarrays is small (less than 4), the *BCE* is exceptionally low.

In response to such problems, this paper proposes a one-step method named Multi-Particle Multi-Parameter Dynamic Weight Particle Swarm Optimization Subarray Partition algorithm (MPMP-DWPSO-SP) based on PSO. The BCE, as the fitness of the MPMP-DWPSO-SP, is computed by the generalized eigenvalue calculation method [12]. The novelty of this paper is that the proposed method is a one-step optimization algorithm, which can simultaneously optimize the position and subarray layout in each iteration, and partitions the subarrays according to the distance of the elements' positions near the center. The planar array model of the Sparse Quadrant Symmetrical Rectangular Array (SQSRA) that we designed presents symmetrical and regular features, which can greatly simplify the feeding network in actual production. Simulations show that the results obtained by using such a one-step optimization method are better than those obtained by the two-step optimization method. When the number of divided subarrays is less than or equal to 4, the *BCE* can still reach about 90%. Moreover, a new model is used to optimize the two subarrays whose *BCE* obtained can reach 91.69%, and the *CSL* is $-17.61$ dB. The method proposed in this paper can greatly reduce the cost and simplify the feeding network, which has important theoretical value for practical applications in the case of requiring a small number of subarrays.

## 2. MATHEMATICAL MODEL OF THE MAXIMUM BCE AND SUBARRAY PARTITION

The model of the SQSRA MWPT system is depicted in Fig. 1. The maximum *BCE* and the method of subarray partition are derived in this section.
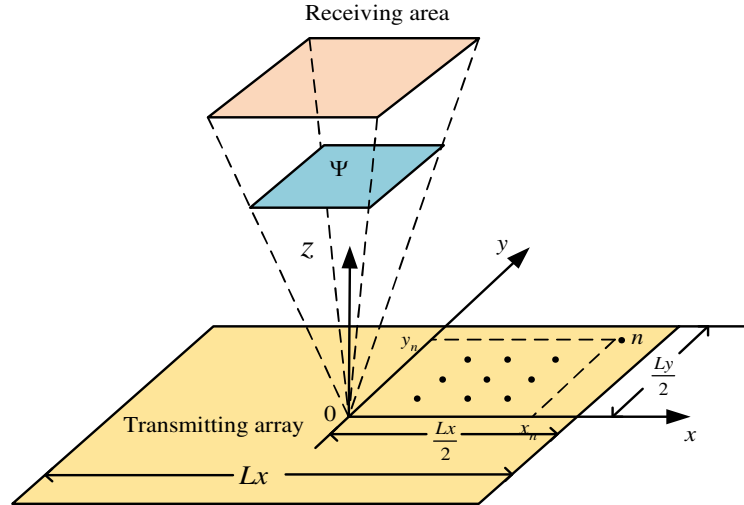


**Figure 1.** The model of the SQSRA MWPT system.

Within this model, we assume that the transmitting array has an aperture of $L_x \times L_y$ and $N = N_x \times N_y$ array elements separately distributed on the $XOY$ plane (Fig. 1 only shows the elements of the first quadrant). The receiving array is in the far-field zone. The rectangular array factor can be expressed as [12]:

$$F(u, v) = \sum_{n=1}^{N} I_n e^{ik(ux_n + vy_n)} \tag{1}$$

where $u = \sin\theta\cos\varphi$ and $v = \sin\theta\sin\varphi$ are angular coordinates; $I_n$ denotes the element excitation

amplitude; $k = 2\pi/\lambda$ represents the wavenumber. $BCE$ can be defined as:

$$BCE \triangleq \frac{P_\Psi}{P_\Omega} = \frac{\int_\Psi |F(u,v)|^2 dudv}{\int_\Omega |F(u,v)|^2 dudv} \tag{2}$$

where $P_{\Psi/\Omega} = \int_{\Psi/\Omega} |F(u,v)|^2 dudv$ denotes the power flowing through the area $\Psi/\Omega$. $\Psi \triangleq \{(u,v) : -u_0 \le u \le u_0, -v_0 \le v \le v_0\}$ and $\Omega \triangleq \{(u,v) : u^2 + v^2 \le 1\}$. According to [12], $BCE$ can be obtained by the method of calculating generalized eigenvalues, which can be expressed as:

$$BCE^{\max} = \left\{ \frac{(W^{\max})^H A (W^{\max})}{(W^{\max})^H B (W^{\max})} \right\} = \eta_{\max} \left\{ \frac{(W^{\max})^H B (W^{\max})}{(W^{\max})^H B (W^{\max})} \right\} = \eta_{\max} \tag{3}$$

where $\eta_{\max}$ is the maximum generalized eigenvalue of $AW^{\max} = \eta_{\max} BW^{\max}$, and $W^{\max}$ is the corresponding eigenvector. $A$ and $B$ are defined as:

$$\begin{cases} A \triangleq \int_\Psi v(u,v) v(u,v)^H dudv \\ B \triangleq \int_\Omega v(u,v) v(u,v)^H dudv \end{cases} \tag{4}$$

where

$$v(u,v) = \left[ e^{-jk(ux_1+vy_1)}, \ldots, e^{-jk(ux_N+vy_N)} \right]^H \tag{5}$$

For more derivation details, readers can refer to [12]. According to [12], $CSL$ (dB) can be written as:

$$CSL(\text{dB}) = 10 \lg \frac{\max_{\theta,\varphi \notin \Psi} |F(\theta,\varphi)|^2}{\max_{\theta,\varphi \in \Omega} |F(\theta,\varphi)|^2} \tag{6}$$

We derive the following equations for partitioning the subarrays according to the distance of the elements' positions near the center. Assume that the vector $D_{distant}$ records the distance from each element to the center, which can be expressed as

$$D_{distant} = \left[ \sqrt{x_1^2 + y_1^2} \quad \sqrt{x_2^2 + y_2^2} \quad \ldots \quad \sqrt{x_N^2 + y_N^2} \right]^T \tag{7}$$

The partition method is shown in Fig. 2.

The radius vector $RR$ can be expressed as:

$$RR = [r_1, r_2, \ldots, r_{M+1}]^T \tag{8}$$

The optimized model for the radius can be expressed as:

$$\begin{cases} find\ RR = [r_1, r_2, \ldots, r_{M+1}]^T \\ maximize\ BCE_{\max}(RR) \\ subject\ (a)\ r_1 = 0 \\ \qquad (b)\ r_{M+1} = \sqrt{2} \cdot \dfrac{L_x}{2} \\ \qquad (c)\ r_i - r_{i-1} \ge \sqrt{2} \cdot d_{\min}, \quad i = \{1, 2, \ldots, M+1\} \\ \qquad (d)\ r_1 < r_2 < \ldots < r_{M+1} \end{cases} \tag{9}$$

Suppose that the sub-matrix partition layout matrix $SR$ is a $N \times M$ matrix, which can be expressed as:

$$SR = \begin{bmatrix} R_{11} & R_{12} & \ldots & R_{1M} \\ R_{21} & R_{22} & \ldots & R_{2M} \\ \vdots & \vdots & \ddots & \vdots \\ R_{N1} & R_{N2} & \ldots & R_{NM} \end{bmatrix} \quad R_{nm} = \begin{cases} 1 & The\ nth\ element \in the\ mth\ subarray \\ 0 & The\ nth\ element \notin the\ mth\ subarray \end{cases} \tag{10}$$
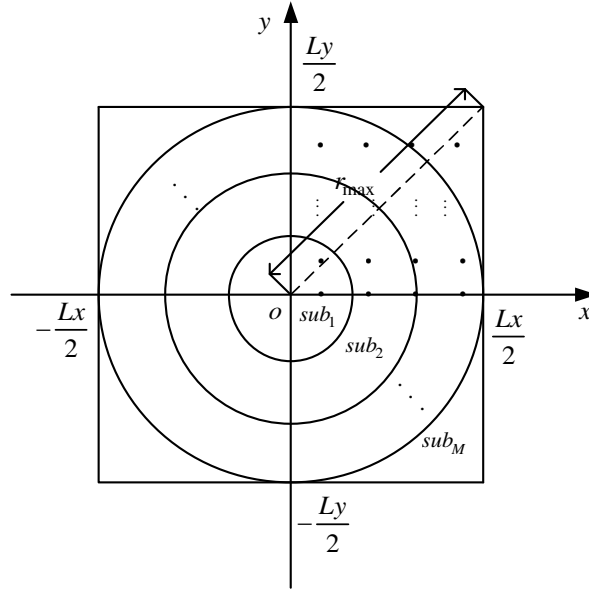$$n = 1, 2, \ldots, N; \quad m = 1, 2, \ldots, M.$$

**Figure 2.** The model of subarray partition radius.

To ensure that each element can only belong to one subarray, the following needs to be met:

$$\sum_{m=1}^{M} R_{nm} = 1, \ (n = 1, 2, \ldots, N) \tag{11}$$

Partition method: if $r_i \leq D_{distant}(n) < r_{i+1}$; $n \in (1, N)$, $i = \{1, 2, \ldots, M\}$, it means: *The nth element in the ith subarray.* Define the initial excitation vector as *weight_initial*:

$$weight\_initial = [w_1, w_2, \ldots, w_N]^T \tag{12}$$

Define the subarray excitation vector as *weight_sub*:

$$weight\_sub = [w\_sub_1, \ w\_sub_2, \ \ldots, \ w\_sub_M]^T \tag{13}$$

The subarray excitation vector can be obtained by multiplying *weight_initial* and *SR* and calculating the arithmetic mean, which can be calculated according to Equation (14):

$$w\_sub_m = \frac{\sum_{n=1}^{N} SR_{nm} \cdot w_n^{initial}}{\sum_{n=1}^{N} SR_{nm}}, \quad (m = 1, 2, \ldots, M) \tag{14}$$

The excitation vector *weight_sub_all* after subarray partition can be obtained as follows:

$$weight\_sub\_all = SR \cdot weight\_sub \tag{15}$$

Then *BCE* can be calculated by Eq. (16):

$$BCE = \frac{weight\_sub\_all^H \cdot A \cdot weight\_sub\_all}{weight\_sub\_all^H \cdot B \cdot weight\_sub\_all} \tag{16}$$

## 3. MPMP-DWPSO-SP AND ITS APPLICATION FOR THE SYNTHESIS OF THE SQSRA

### 3.1. Description of MPMP-DWPSO-SP

The following is a process description for the optimization method MPMP-DWPSO-SP. We assume that $N$, $M$, $L_x \times L_y$, $\Psi$, and $(x_n, y_n)$, respectively, denote the number of array elements, the number

of subarrays, array aperture, receiving area, and the position of the array element. $vx$ and $vr$ represent the updated velocity of the position and radius. The values of $BCE^1$ and $BCE^2$, respectively, represent the initialized $BCE$ and the $BCE$ obtained after subarray partition. $pbest$ represents the local optimal extremum, and $gbest$ represents the global optimal extremum. $pbest\_x$ and $gbest\_x$, respectively, represent the positions corresponding to $pbest$ and $gbest$. $rpbest$ and $rgbest$ represent the radii corresponding to $pbest$ and $gbest$.

**Step 1:** Initialize $N$, $M$, $L_x \times L_y$, $\Psi$, $(x_n, y_n)$, $vx$, $vr$, etc.

**Step 2:** Calculate $BCE^1$ in Eq. (3), $weight\_sub$ in Eq. (14), and $BCE^2$ in Eq. (16).

**Step 3:** Calculate $pbest$ and $gbest$.

**Step 4:** Update $(x_n, y_n)$, $vx$ and $vr$ of each particle according to Eqs. (17)–(21).

The dynamic weight expression is as follows:

$$w = w_{\max} - (w_{\max} - w_{\min}) \cdot (1 - i/T)^2 \tag{17}$$

where $i$ represents the current number of iterations, and $T$ represents the maximum number of iterations. The inertia weight indicates how much the original velocity is retained. Larger weights are conducive to global search, and smaller weights are conducive to local search. The use of dynamic weights can converge more quickly and is conducive to searching for the optimal value. This simulation has been simulated by the Monte Carlo method many times. When $w$ attenuates from 0.9 to 0.4, the algorithm has the strongest searchability. The weight curve can be expressed in Fig. 3. $vx$, $vr$, and position update expressions are as follows:

$$vx_{i+1} = w \times vx_i + c_1 \times rand \times (pbest\_x_i - x_i) + c_2 \times rand \times (gbest\_x_i - x_i) \tag{18}$$
$$x = x + vx_{i+1} \tag{19}$$
$$vr_{i+1} = w \times vr_i + c_1 \times rand \times (rpbest_i - r_i) + c_2 \times rand \times (rgbest_i - r_i) \tag{20}$$
$$r_{i+1} = r_i + vr_{i+1} \tag{21}$$

where $c_1$ and $c_2$ are the learning factors of the particle for its optimal solution and the group's optimal solution. The velocity update equation is principally composed of three parts. The first part is the current velocity; the second part is the learning of the optimal solution currently searched by the particle; and the third part is the learning of the optimal solution of the group search. Through the learning of the last two parts, particles can quickly converge to the optimal solution in the global scope. At the beginning of the PSO, due to the need to quickly search for the global content, its velocity component accounts for a large proportion, and in the later stage of the algorithm, due to the search within the optimal area, the proportion of its velocity component should be decreased. Therefore, the use of dynamic weights is more conducive to finding the optimal value.
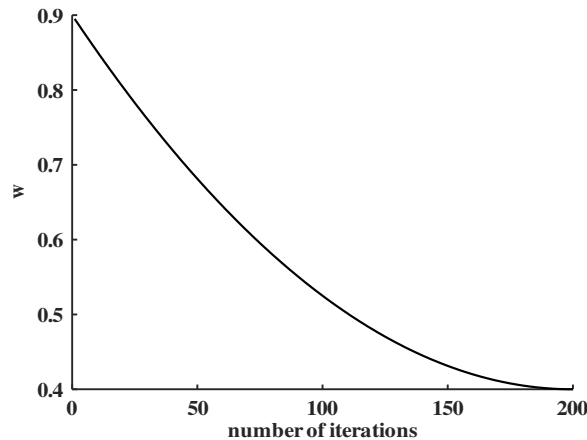


**Figure 3.** Dynamic non-linear decreasing weight curve.

**Step 5:** Calculate $BCE^2$ again, and select the best individual (*pbest* and *gbest*).

**Step 6:** Judge whether to update *pbest* and *gbest*, if the fitness value of the current particle is greater than *pbest* and *gbest*, then update, otherwise keep.

**Step 7:** Judge whether $T$ is satisfied, return to step 4 if not satisfied, else output *gbest*.

After the above steps, the maximum $BCE$ after the subarray partition can be achieved. The pseudo-code can be expressed in Fig. 4. *NP* represents the maximum number of particles in the group.

Through the pseudo code, we can conclude that our proposed method is a one-step method, which optimizes the position and subarray layout structure at the same time in each iteration.

## 3.2. The Synthesis of the SQSRA by Using MPMP-DWPSO-SP

The optimization model of using the MPMP-DWPSO-SP algorithm to optimize SQSRA can be expressed as:

$$
\begin{cases}
find\ [X, Y, RR] = [x_1, x_2, \ldots, x_N,\ y_1, y_2, \ldots, y_N,\ r_1, r_2, \ldots, r_{M+1}]^H \\
maximize\ BCE_{\max}\left([X, Y, RR]\right) \\
subject\ (a)\ (x_n, y_n) = \left(-x_{n-N/4}, y_{n-N/4}\right),\quad n = \left\{\dfrac{N}{4}+1, \ldots, \dfrac{N}{2}\right\}; \\
\quad\quad (b)\ (x_n, y_n) = (-x_{n-N/2}, -y_{n-N/2}),\quad n = \left\{\dfrac{N}{2}+1, \ldots, \dfrac{3N}{4}\right\}; \\
\quad\quad (c)\ (x_n, y_n) = (x_{n-3N/4}, -y_{n-3N/4}),\quad n = \left\{\dfrac{3N}{4}+1, \ldots, N\right\}; \\
\quad\quad (d)\ dmin/2 < x_n < L_x/2,\quad n = \left\{1, 2, \ldots, \dfrac{N}{4}\right\}; \\
\quad\quad (e)\ dmin/2 < y_n < L_y/2,\quad n = \left\{1, 2, \ldots, \dfrac{N}{4}\right\}; \\
\quad\quad (f)\ \sqrt{(x_i - x_j)^2 + (y_i - y_j)^2} \geq dmin,\quad i, j \in \{1, 2, \ldots, N\},\quad i \neq j; \\
\quad\quad (g)\ \left(x_{N/4}, y_{N/4}\right) = (L_x/2, L_y/2) \\
\quad\quad (h)\ 0 < r_i \leq \sqrt{2} \cdot L_x/2,\quad i = \{1, 2, \ldots, M+1\} \\
\quad\quad (i)\ r_{i+1} - r_i \geq \sqrt{2} \cdot dmin,\quad i = \{1, 2, \ldots, M\} \\
\quad\quad (j)\ r_1 = 0,\quad r_{M+1} = \sqrt{2} \cdot L_x/2
\end{cases}
\tag{22}
$$

The optimization goal of this model is to improve the $BCE$ as much as possible. The optimization variables are the position of the element and the radius vector of the subarray. Consequently, the proposed MPMP-DWPSO-SP is one-step optimization algorithm, which can simultaneously optimize the position and subarray layout, so that global optimal solution is obtained. Only the first quadrant is optimized. The position coordinates of the other quadrants can be obtained by symmetry.

## 4. SIMULATIONS AND RESULTS

In this section, the effectiveness and efficiency of the MPMP-DWPSO-SP method in dealing with different planar models will be evaluated from four aspects. Firstly, we used the proposed method to optimize three planar array models. The first planar array model is SQSRA. Such a regular array can simplify the feeding network and reduce the manufacturing cost in practical applications. The second planar array model is a Nonuniform Distributed Rectangular Planar Array (NDRPA), such an overall model has higher optimization freedom and may get better results. If readers want to know the physical model of NDRPA, you can refer to the model of SNANDPA in [9]. The third array model optimizes only the globally optimal individuals (only-gbest) in SQSRA. This optimization can directly test the effectiveness of the method proposed in this paper. Secondly, we compared these three models by using the one-step method with other different planar array models by using the previous two-step method in

```
The pseudo-code of the MPMP-DWPSO-SP method
```

<div>

The pseudo-code of the MPMP-DWPSO-SP method

Initialization parameters

For $NP\_count = 1{:}NP$

    Calculate $BCE^1$ and $weight\_initial$ according to (3).

    Calculate the $SR$ according to distance partition method.

    Calculate $W\_sub$ according to (14).

    Calculate $BCE^2$ according to (16).

End

Select the individual with the maximum $BCE^2$ as $pbest$.

Record global optimal value $gbest$.

 For $i = 1{:}T$

    For $NP\_count = 1{:}NP$

        Update the velocity and position of particles according to (17)–(21)

        Calculate $BCE^1$ and $weight\_initial$ according to (3).

        Calculate the $SR$ according to distance partition method.

        Calculate $W\_sub$ according to (14).

        Calculate $BCE^2$ after subarray partition according to (16).

        If $BCE^2 > pbest$

            $pbest = BCE^2$

        End

    End

    Select the maximum $BCE^2$ among all particles as $gbest$.

End

Output $gbest$, optimal $SR$, optimal $W\_sub$, etc.

</div>

**Figure 4.** The pseudo-code of the MPMP-DWPSO-SP.

synthesis performance. Thirdly, we compared our proposed method with another three PSO methods in array performance under the same conditions. At last, we designed an intelligent optimization model for partitioning two subarrays. The CPU used in all simulations is Intel(R) Core (TM) i7-10750H at 2.60 GHz, with 16 GB RAM, and the simulation software is MATLAB R2019a in this paper.

We use $BCE$ and $CSL$ as two performance indicators to test the effectiveness of the proposed method. The maximum number of iterations $(T)$ in all simulations is set to 200, and the number of particles $(NP)$ is set to 50. The receiving area is set to $u_0 = v_0 = 0.2$. In the MPMP-PSO-SP algorithm, the learning factors $c_1$ and $c_2$ are set to 2, the wavelength $\lambda$ set to 1, and the minimum array element spacing $d_{\min}$ set to 0.5.
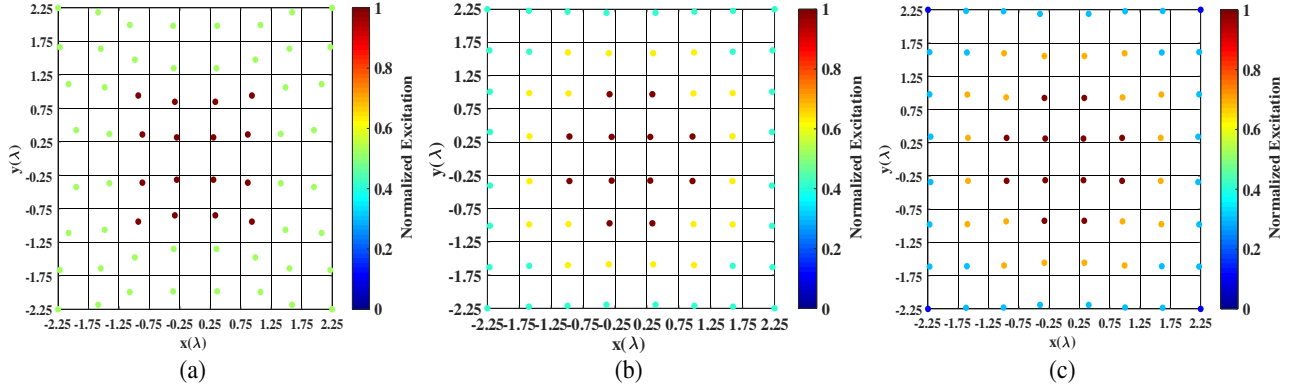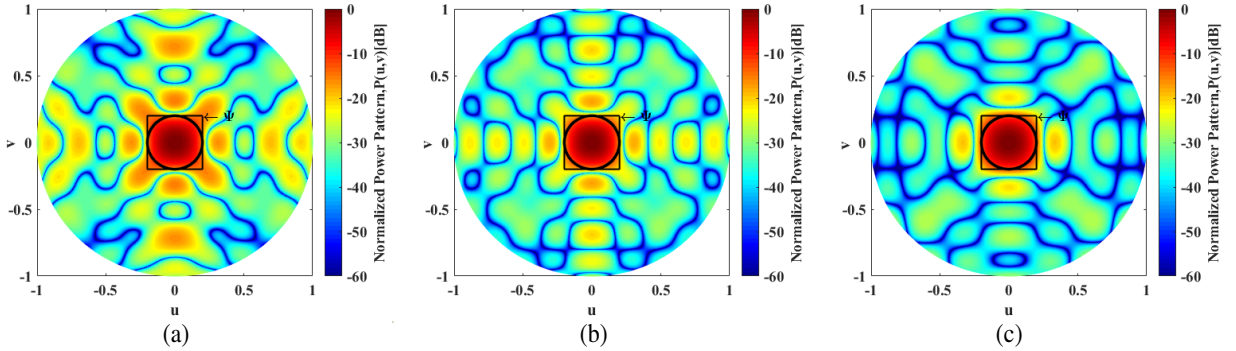
## 4.1. Results of Three Models by Using MPMP-DWPSO-SP

The first set of simulations involves the synthesis of the SQSRA model with an aperture of $4.5\lambda \times 4.5\lambda$ and $N = 8 \times 8$ elements. The results of the SQSRA by using MPMP-DWPSO-SP are recorded in Table 1. The excitation position layout and normalized power pattern of different subarrays are shown in Fig. 5 and Fig. 6.

From Table 1, Fig. 5, and Fig. 6, we can know that the $BCE$ can reach more than 90% $(BCE|_{SQSRA}^{M=4} = 92.96\%)$ when SQSRA of more than 3 subarrays is optimized by using the MPMP-DWPSO-SP algorithm. Different colors in Fig. 5 represent different subarrays, and the excitation of each subarray is the same. So, the number of amplifiers required is determined by the number of subarrays, which can greatly reduce the cost. Most of the energy in the power pattern in Fig. 6 is concentrated in the central receiving area, thus showing good array performance.

**Table 1.** Synthesis results of SQSRA by using MPMP-DWPSO-SP method.

| $N_x = N_y$ | $N$ | $M$ | $u_0 = v_0$ | $W\_sub$ | $BCE/\%$ | $CSL/\mathrm{dB}$ |
|:---:|:---:|:---:|:---:|:---:|:---:|:---:|
| $8 \times 8$ | 64 | 2 | 0.2 | 0.7804, 0.4106 | 89.72 | $-15.19$ |
| $8 \times 8$ | 64 | 3 | 0.2 | 0.9146, 0.5778, 0.3824 | 91.37 | $-17.64$ |
| $8 \times 8$ | 64 | 4 | 0.2 | 0.9343, 0.6490, 0.2859, 0.0945 | 92.96 | $-13.18$ |



**Figure 5.** Subarray configurations obtained for SQSRA model by using MPMP-DWPSO-SP when (a) $M = 2$, (b) $M = 3$, (c) $M = 4$ ($L_x = L_y = 4.5$, $u_0 = v_0 = 0.2$, $N = 8 \times 8$).



**Figure 6.** Normalized power pattern obtained for SQSRA model by using MPMP-DWPSO-SP when (a) $M = 2$, (b) $M = 3$, (c) $M = 4$ ($L_x = L_y = 4.5$, $u_0 = v_0 = 0.2$, $N = 8 \times 8$).

The second set of simulations involves the synthesis of the NDRPA model with an aperture of $4.5\lambda \times 4.5\lambda$ and $N = 8 \times 8$ elements. The results of the NDRPA by using the MPMP-DWPSO-SP are recorded in Table 2. The excitation position layout and normalized power pattern of four subarrays are shown in Fig. 7.

**Table 2.** Synthesis results of NDRPA by using MPMP-DWPSO-SP method.

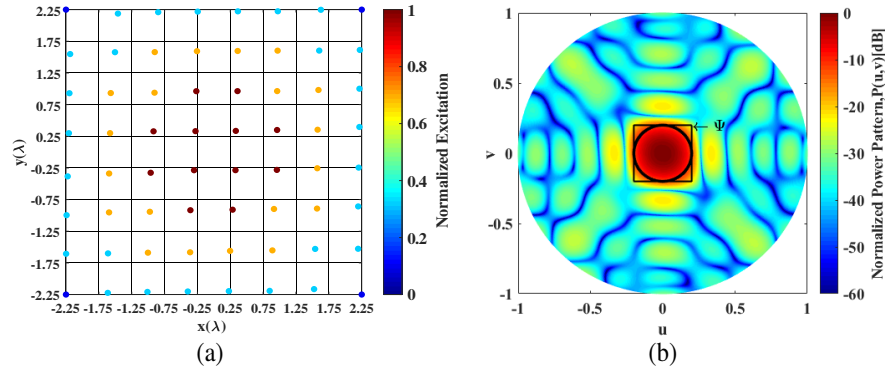| $N_x = N_y$ | $N$ | $M$ | $u_0 = v_0$ | $W\_sub$ | $BCE/\%$ | $CSL/\mathrm{dB}$ |
|:---:|:---:|:---:|:---:|:---:|:---:|:---:|
| $8 \times 8$ | 64 | 2 | 0.2 | 0.7202, 0.2682 | 86.52 | $-14.17$ |
| $8 \times 8$ | 64 | 3 | 0.2 | 0.6940, 0.3162, 0.1473 | 88.53 | $-14.13$ |
| $8 \times 8$ | 64 | 4 | 0.2 | 0.8708, 0.6009, 0.2722, 0.0940 | 93.04 | $-12.84$ |

**Figure 7.** Simulation results of the NDRPA model ($BCE = 93.04\%$, $CSL = -12.84\,\text{dB}$) (a) layout and excitation, (b) normalized power pattern. ($L_x = L_y = 4.5$, $u_0 = v_0 = 0.2$, $N = 8 \times 8$, $M = 4$).

From Table 2 and Fig. 7, we can know that $BCE$ can reach more than 90% ($BCE|_{NDRPA}^{M=4} = 93.04\%$) when NDRPA of four subarrays is optimized by using the MPMP-DWPSO-SP algorithm. Through the comparison of Table 1 and Table 2, we know that NDRPA has a higher degree of freedom in optimization and obtains a better $BCE$ when dividing 4 subarrays.

In the third simulation, we only divide the global optimum (only-gbest) searched by the MPMP-DWPSO-SP and calculate the $BCE$. The results are recorded in Table 3. The excitation position layout and normalized power pattern of four subarrays are shown in Fig. 8.

**Table 3.** Synthesis results of only-gbest by using MPMP-DWPSO-SP method.

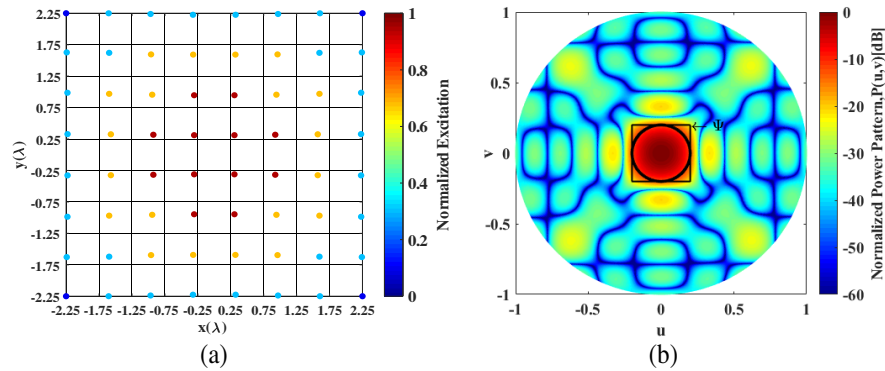| $N_x = N_y$ | $N$ | $M$ | $u_0 = v_0$ | $W\_sub$ | $BCE/\%$ | $CSL/\text{dB}$ |
|---|---|---|---|---|---|---|
| $8 \times 8$ | 64 | 2 | 0.2 | 0.8708, 0.3606 | 87.64 | $-14.37$ |
| $8 \times 8$ | 64 | 3 | 0.2 | 0.9607, 0.7140, 0.3006 | 90.76 | $-13.55$ |
| $8 \times 8$ | 64 | 4 | 0.2 | 0.9478, 0.6760, 0.3002, 0.1080 | 92.70 | $-13.39$ |



**Figure 8.** Simulation results of the only-gbest model ($BCE = 92.70\%$, $CSL = -13.39\,\text{dB}$) (a) layout and excitation, (b) normalized power pattern. ($L_x = L_y = 4.5$, $u_0 = v_0 = 0.2$, $N = 8 \times 8$, $M = 4$).

Through the above three simulations, it can be known that whether it is to optimize SQSRA, NDRPA, or only-gbest, the results of the $BCE$ obtained by the subarray partition algorithm are all about 90% ($BCE|_{only\text{-}gbest}^{M=4} = 92.70\%$), indicating that the method is effective for the problem of too low $BCE$ caused by a small number of subarrays.

## 4.2. Comparison with Other Planar Arrays in BCE

To further illustrate the effectiveness of the MPMP-DWPSO-SP algorithm, we compared the results of optimizing the three models by using the one-step method with SNANDPA by using the previous two-step method in [9]. The comprehensive comparison result is shown in Fig. 9.
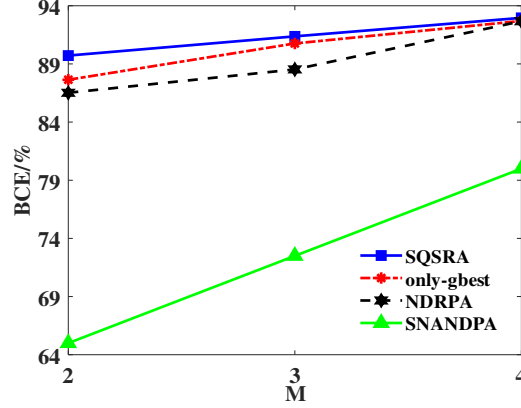


**Figure 9.** Comparison results of three models and SNANDPA.

From Fig. 9 we can prove that the algorithm can greatly improve the $BCE$ for optimizing a small number of subarrays. Compared with SNANDPA, $BCE$ increased by nearly 20% ($BCE|_{SQSRA}^{M=2} = 89\%$ vs. $BCE|_{SNANDPA}^{M=2} = 65\%$), which verifies the significant advantages of the MPMP-DWPSO-SP algorithm in the process of optimizing a small number of subarrays.

To further verify the effectiveness of this method, we compare six array models by using several comprehensive performance indicators such as $BCE$ and $CSL$. $\gamma_a$ and $\gamma_e$ compare three different array models. $\gamma_a$ and $\gamma_e$, respectively, represent amplifier sparsity and element sparsity of the transmitting array defined as:

$$\gamma_a = \frac{M}{N} \tag{23}$$

$$\gamma_e \triangleq \frac{N}{N_{full}} \tag{24}$$

where $N_{full}$ represents the number of fully populated array elements. The comprehensive comparison results are shown in Table 4.

**Table 4.** Comparison results of three models and other array models.

|  | Ref. [12] | Ref. [9] | Ref. [13] | SQSRA | NDRPA | only-gbest |
|---|---|---|---|---|---|---|
| $N$ | 100 | 64 | 100 | 64 | 64 | 64 |
| $M$ | 1 | 6 | 1 | 4 | 4 | 4 |
| $\gamma_e(\%)$ | 100 | 64 | 100 | 64 | 64 | 64 |
| $\gamma_a(\%)$ | 1 | 9.4 | 1 | 6.25 | 6.25 | 6.25 |
| $BCE$ (%) | 86.48 | 91.09% | 91.06 | 92.96% | 93.04 | 92.70 |
| $CSL$ (dB) | $-7.78$ | $-14.68$ | $-16.01$ | 13.18 | $-12.84$ | 13.39 |

According to Table 4, it can be concluded that the $BCE$ achieved by the proposed method is 1.95% higher than the result in [9] ($BCE|_{NDRPA} = 93.04\%$ vs. $BCE|_{[9]} = 91.09\%$). Although the array in [13] is a fully populated and uniformly excited array ($\gamma_a = 1$), the $BCE$ only reaches 91%. The proposed method can achieve the $BCE$ of 93.04% by dividing only 4 subarrays, which can greatly reduce the cost and obtain higher $BCE$.

### 4.3. MPMP-DWPSO-SP Method Performance Compared to Different PSO Algorithm

To verify that the effect of the algorithm is better, we have compared different types of PSO [14–16], as shown in Fig. 10.
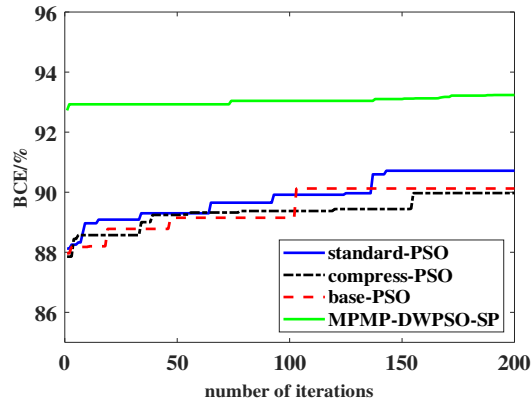


**Figure 10.** Simulation results of the different PSO algorithm.

Through Fig. 10, we can conclude that our proposed method MPMP-DWPSO-SP is better than basic PSO [14], standard PSO [15], and compression factor PSO [16]. We found that the iteration trace of the MPMP-DWPSO-SP was relatively smooth, and the algorithm could converge quickly. Compared with MPMP-DWPSO-SP, the $BCE$ of the standard PSO, the compression factor PSO, and the basic PSO are lower, and the convergence speed is slower. The basic PSO algorithm does not consider the relationship between global optimization and local optimization. The compression factor PSO ignores the influence of inertia weights on optimization; therefore, the algorithm converges slowly and falls into local optima. The standard PSO allows linear adjustment of inertia weights, global optimization weights, and local optimization weights. Therefore, the standard PSO has a better fitness value. The MPMP-DWPSO-SP algorithm uses nonlinear dynamic weights. The initial global search ability is strong, and the later local search ability is strong, so the optimal value $BCE$ is much higher.

### 4.4. The Other Intelligent Optimal Model in Optimizing Two Subarrays

For the problem that the $BCE$ of partitioning two subarrays does not reach more than 90%, and the other model by using MPMP-DWPSO-SP algorithm suitable for optimizing two subarrays is proposed,
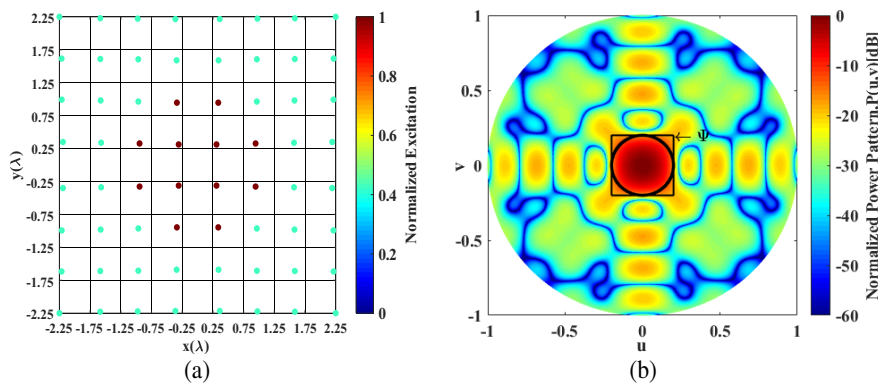


**Figure 11.** Simulation results of the intelligence optimal model ($BCE = 91.69\%$, $CSL = -17.61\,\text{dB}$) (a) layout and excitation, (b) normalized power pattern. ($L_x = L_y = 4.5$, $u_0 = v_0 = 0.2$, $N = 8 \times 8$, $M = 2$).

which can be expressed as formula (25):

$$
\begin{cases}
find\ [X, Y, RR] = [x_1, x_2, \ldots, x_N,\ y_1, y_2, \ldots, y_N,\ r_1, r_2, \ldots, r_{M+1}]^H \\[4pt]
maximize\ BCE_{\max}\left([X, Y, RR]\right) \\[4pt]
subject\ (a)\ (x_n, y_n) = \left(-x_{n-N/4}, y_{n-N/4}\right), \quad n = \left\{\dfrac{N}{4}+1, \ldots, \dfrac{N}{2}\right\}; \\[10pt]
\qquad\ (b)\ (x_n, y_n) = (-x_{n-N/2}, -y_{n-N/2}), \quad n = \left\{\dfrac{N}{2}+1, \ldots, \dfrac{3N}{4}\right\}; \\[10pt]
\qquad\ (c)\ (x_n, y_n) = (x_{n-3N/4}, -y_{n-3N/4}), \quad n = \left\{\dfrac{3N}{4}+1, \ldots, N\right\}; \\[10pt]
\qquad\ (d)\ dmin/2 < x_n < L_x/2, \quad n = \left\{1, 2, \ldots, \dfrac{N}{4}\right\}; \\[10pt]
\qquad\ (e)\ dmin/2 < y_n < L_y/2, \quad n = \left\{1, 2, \ldots, \dfrac{N}{4}\right\}; \\[10pt]
\qquad\ (f)\ \sqrt{(x_i - x_j)^2 + (y_i - y_j)^2} \geq dmin, \quad i, j \in \{1, 2, \ldots, N\}, \quad i \neq j; \\[6pt]
\qquad\ (g)\ \left(x_{N/4}, y_{N/4}\right) = (L_x/2, L_y/2) \\[4pt]
\qquad\ (h)\ 0 < r_i \leq L_x/2, \quad i = \{2, 3, \ldots, M\} \\[4pt]
\qquad\ (i)\ r_{i+1} - r_i \geq dmin, \quad i = \{1, 2, \ldots, M-1\} \\[4pt]
\qquad\ (j)\ r_1 = 0, \quad r_M = L_x/2, \quad r_{M+1} = \sqrt{2} \cdot L_x/2
\end{cases}
\tag{25}
$$

The difference between models (22) and (25) is that the radius spacing is set to $dmin$, and the maximum number of subarrays is set to 4. In this way, the intelligent optimization finds the subarrays and obtains the results of two subarrays as shown in Table 5. The excitation position layout and normalized power pattern of the two subarrays are shown in Fig. 11.

**Table 5.** Synthesis results of the intelligence model.

| $N_x = N_y$ | $N$ | $M$ | $u_0 = v_0$ | $W\_sub$ | $BCE/\%$ | $CSL/\mathrm{dB}$ |
|:---:|:---:|:---:|:---:|:---:|:---:|:---:|
| $8 \times 8$ | 64 | 2 | 0.2 | 0.9344, 0.4075 | 91.69 | $-17.61$ |

The results in Table 5 verify that the model is effective for optimizing two subarrays, and the $BCE$ is increased to more than 90%. This requires only two amplifiers, which greatly reduces the cost and simplifies the feeding.

## 5. CONCLUSION

In this paper, aiming at the problem of too low $BCE$ caused by partitioning a small number of subarrays, an effective one-step method, named MPMP-DWPSO-SP, is proposed to solve this problem. The MPMP-DWPSO-SP integrates DWPSO and subarray partition technology and improves the array performance by simultaneously optimizing the subarray structure and position of the array elements. The algorithm divides the subarray according to the distance from the position of the element to the center, and updates multiple parameters at the same time, which is more conducive to searching for the optimal individual in the group. In particular, a new intelligent optimization model is proposed, when dividing two subarrays. By performing a series of simulations and comparing the results of the MPMP-DWPSO-SP with those of other algorithms in [9, 12, 13], it is concluded that in the case of dividing a small number of subarrays, the proposed algorithm is more effective and gains lower sparse rate and higher $BCE$ than other algorithms.

## ACKNOWLEDGMENT

## REFERENCES

1. Lu, F., H. Zhang, W. Li, et al., "A high-efficiency and long-distance power-relay system with equal power distribution," *IEEE Journal of Emerging and Selected Topics in Power Electronics*, Vol. 8, No. 2, 1419–1427, 2020.

2. Li, Y. and V. Jandhyala, "Design of retrodirective antenna arrays for short-range wireless power transmission," *IEEE Transactions on Antennas and Propagation*, Vol. 60, No. 1, 206–211, 2012.

3. Massa, A., G. Oliveri, F. Viani, and P. Rocca, "Array designs for long-distance wireless power transmission: State-of-the-art and innovative solutions," *Proceedings of the IEEE*, Vol. 101, No. 6, 1464–1481, 2013.

4. Li, X., B. Duan, L. Song, et al., "A new concept of space solar power satellite," *Acta Astronaut*, Vol. 136, 182–189, 2017.

5. Li, X., J. Zhou, B, Duan, et al., "Performance of planar arrays for microwave power transmission with position errors," *IEEE Antennas Wireless Propagation Letters*, Vol. 14, 1794–1797, 2015.

6. Xiong, Z., Z. Xu, S. Chen, et al., "Subarray partition in array antenna based on the algorithm X," *IEEE Antennas & Wireless Propagation Letters*, Vol. 12, No. 12, 906–909, 2013.

7. Liu, X., X. Zhang, and H. Yan, "Research of subarray partition in optically phased array radar," *Applied Science & Technology*, 2006.

8. Li, X., B. Duan, and L. Song, "Design of clustered planar arrays for microwave wireless power transmission," *IEEE Transactions on Antennas and Propagation*, Vol. 67, No. 1, 606–611, 2019.

9. Li, J. and S. Chang, "Novel sparse planar array synthesis model for microwave power transmission systems with high efficiency and low cost," *Progress In Electromagnetics Research C*, Vol. 115, 245–259, 2021.

10. Li, J., J. Pan, and X. Li, "A novel synthesis method of sparse nonuniform-amplitude concentric ring arrays for microwave power transmission," *Progress In Electromagnetics Research C*, Vol. 107, 1–15, 2021.

11. Haupt, R. L., "Optimized element spacing for low sidelobe concentric ring arrays," *IEEE Transactions on Antennas and Propagation*, Vol. 56, No. 1, 266–268, 2008.

12. Oliveri, G., L. Poli, and A. Massa, "Maximum efficiency beam synthesis of radiating planar arrays for wireless power transmission," *IEEE Transactions on Antennas and Propagation*, Vol. 61, No. 5, 2490–2499, 2013.

13. Li, X., B. Duan, J. Zhou, et al., "Planar array synthesis for optimal microwave power transmission with multiple constraints," *IEEE Antennas Wireless Propagation Letters*, Vol. 16, 70–73, 2017.

14. Poli, R., J. Kennedy, and T. Blackwell, "Particle swarm optimization," *Swarm Intelligence*, Vol. 1, No. 1, 2007.

15. Miao, A., X. Shi, J. Zhang, et al., "A modified particle swarm optimizer with dynamical inertia weight," *Fuzzy Information and Engineering Volume 2. Advances in Intelligent and Soft Computing*, Vol. 62, 767–776, 2009.

16. Clerc, M. and J. Kennedy, "The particle swarm-explosion, stability, and convergence in a multidimensional complex space," *IEEE Transactions on Evolutionary Computation*, Vol. 6, No. 1, 58–73, 2002.